Int J Clin Exp Pathol 2016;9(2):1127-1137
www.ijcep.com /ISSN:1936-2625/IJCEP0020065

Original Article

MicroRNA expression patterns of ankle synovial tissues in rats with monosodium urate crystal-induced gouty arthritis

Ying Xie[1], Jieru Han[2], Fei Chen[1], Jiayi Chang[1], Bing Wang[3], Fuzhen Li[1], Xutao Sun[1], Deyou Jiang[1]

[1]Department of Synopsis of The Golden Chamber, School of Basic Medical Sciences, Heilongjiang University of Chinese Medicine, Harbin, People's Republic of China; [2]Department of Seasonal Febrile Diseases, School of Basic Medical Sciences, Heilongjiang University of Chinese Medicine, Harbin, People's Republic of China; [3]Department of The Inner Canon of Huangdi, School of Basic Medical Sciences, Heilongjiang University of Chinese Medicine, Harbin, People's Republic of China

Received November 18, 2015; Accepted January 24, 2016; Epub February 1, 2016; Published February 15, 2016

Abstract: Gout is a common inflammatory arthritis caused by the precipitation of monosodium urate (MSU) crystals. MicroRNAs (miRNAs) are non-coding RNAs that silence genes' expression by binding to their mRNAs. This study was conducted to identify miRNAs implicated in the pathogenesis of gouty arthritis (GA). Acute GA was induced in rats by injecting MSU crystal solution directly into their left ankle joint cavity. The miRNA expression patterns in ankle synovial tissues of control and GA rats were analyzed with Affymetrix miRNA 4.0 microarrays. Seven miRNAs with fold change (FC) > 1.2 and *P* value < 0.05 (unpaired *t* test) were identified. After validation via quantitative real-time PCR, rno-miR-328b-3p, rno-miR-375-5p and rno-miR-299a-5p were confirmed as the upregulated miRNAs in GA rats, while rno-miR-203a-3p, rno-miR-3085 and rno-miR-19b-2-5p were the downregulated ones. Target genes of the six validated miRNAs were predicted with miRDB online database. Results of gene ontology (GO) analysis indicated that genes targeted by the upregulated miRNAs were mainly enriched in transcriptional regulation and negative/positive regulation of apoptotic process, while those targeted by the downregulated miRNAs were annotated into transcriptional regulation and signal transduction. Furthermore, the most significant signaling transduction pathway mediated by the upregulated miRNAs was p53 pathway, a well-known apoptosis related pathway. The downregulated miRNA-targeted genes were enriched in several inflammation or oxidative stress related pathways, such as MAPK and FoxO signaling pathways. Collectively, the identified differentially expressed miRNAs hold the potential to serve as therapeutic molecules or targets for GA.

Keywords: Gouty arthritis, monosodium urate crystals, microRNA, inflammation, apoptosis

Introduction

Gout is a crystal deposition disease, leading to activity limitation or disability in patients if untreated [1, 2]. The final product of purine metabolism, uric acid, has long been recognized as the cause of gouty arthritis (GA) [3]. New therapeutic agents targeting inflammation (interleukin-1β, IL-1β) and lowering urate are currently under investigation [4, 5]. Colchicine and non-steroidal anti-inflammatory drugs are effective for GA management. However, their adverse effects on kidney or cardiovascular system make the treatment of GA challenging [6, 7]. New developments in therapy for GA require for further understanding on its pathogenesis.

MicroRNAs (miRNAs) as small non-coding RNAs assemble with Argonaute (Ago) proteins as miRNA-induced silencing complexes, recognize to their complementary mRNAs, and lead to mRNA deadenylation, decapping and 5'-to-3' degradation [8, 9]. Reportedly, dysregulation of miRNAs occurs across many inflammatory conditions, including rheumatoid arthritis (RA) [10] and osteoarthritis (OA) [11]. Interestingly, recent studies also reveal the implication of miRNAs in GA. MiR-146a expression is decreased in mouse peritoneal monocytes exposed to mono-

sodium urate (MSU) crystals during the acute inflammatory response, and its overexpression can inhibit the MSU crystal-induced overproduction of proinflammatory cytokines in monocytic THP-1 cells [12]. In contrast to miR-146a, miR-155 is highly enriched in peripheral blood and synovial samples derived from GA patients, and its elevation aggravates MSU crystal-induced inflammation [13]. These earlier findings suggest that miRNAs may act as regulators in GA pathogenesis in discrepant ways, and that targeting miRNAs may be a promising strategy for GA treatment. Identifying more novel miRNAs implicated in GA pathogenesis will help to understand how GA develops.

MSU crystals interacting with the surface of cells trigger a variety of cellular signals involved in GA inflammation [7]. Therefore, in this study, MSU crystals were utilized to induce acute GA in rats. By using miRNA microarrays, we compared the miRNA expression in synovial tissues from GA and control rats. The possible targets of the differentially expressed miRNAs were predicated with miRDB database, and further subjected to bioinformatics analysis.

Materials and methods

Animals

Wistar rats (200 ± 20 g) obtained from Vital River Laboratory Animal Technology Co. Ltd (Beijing, China) were housed under controlled conditions (a 12-h light/dark cycle with the temperature of 22 ± 1°C and humidity of 40-60%), and fed with standard laboratory diets. All animal procedures were approved by Animal Care Ethics and Use Committee of Heilongjiang University of Chinese Medicine.

Establishment of MSU crystal-induced GA model in rats

MSU crystals were used to induce acute GA in rats (n = 3 per group). In short, rats were anesthetized with 10% chloral hydrate (3.5 mL/kg; intraperitoneal injection), and then 50 μL MSU solution (20 mg/mL) was injected into their left ankle joint cavity (GA group). Rats in control group were given an equal volume of PBS (Control group). Twenty-four hours later, the blood samples were collected from these rats, and their left ankle circumferences were measured. Thereafter, all rats were sacrificed, and their left ankle synovial tissues were removed and stored in liquid nitrogen.

Total RNA extraction and raw data analysis

Total RNAs were isolated from the synovial tissues and quantified on NanoDrop ND-2100 (Thermo Scientific, Pittsburgh, PA, USA). RNA integrity of each sample was measured on Agilent 2100 (Agilent Technologies, Santa Clara, CA, USA). The RNAs were tailed with Poly A and then labeled with Biotin before hybridizing onto the Affymetrix miRNA 4.0 microarrays that containing 728 mature rat miRNAs. After washing, the arrays were scanned by the Affymetrix Scanner 3000 (Affymetrix) according to the manufacturer's standard protocols. Raw data were exported by analyzing array images with Affymetrix GeneChip Command Console software (Version 4.0).

Quantitative real-time PCR (qRT-PCR) analysis

The miRNA expression levels were further confirmed via qRT-PCR analysis. Samples used in microarray analysis were also used in qRT-PCR analysis. U6 was served as control for miRNA. Threshold cycle method was performed to determine the relative miRNA expression levels. Where appropriate, unpaired *t* test was performed to compare the data using SPSS (Version 20.0).

Microarray data analysis

Microarray raw data were first normalized with RMA, and then analyzed with Genespring software package (Version 12.5; Agilent Technologies). MiRNAs with the absolute fold change (FC) > 1.2 (GA vs. Control group) and P value < 0.05 (unpaired t test) were considered as differentially expressed miRNAs. MiRDB online prediction software was used to predict the possible targets of miRNAs. Principal component analysis (PCA) was performed using the microarray data, and unsupervised hierarchical clustering was performed to show the miRNA expression patterns. Furthermore, gene ontology (GO) and Kyoto encyclopedia of genes and genomes (KEGG) pathway analysis were applied to defining the roles of target genes in GA pathogenesis. A GO or KEGG term with P value < 0.05 was considered as significant (unilateral Fisher exact test).

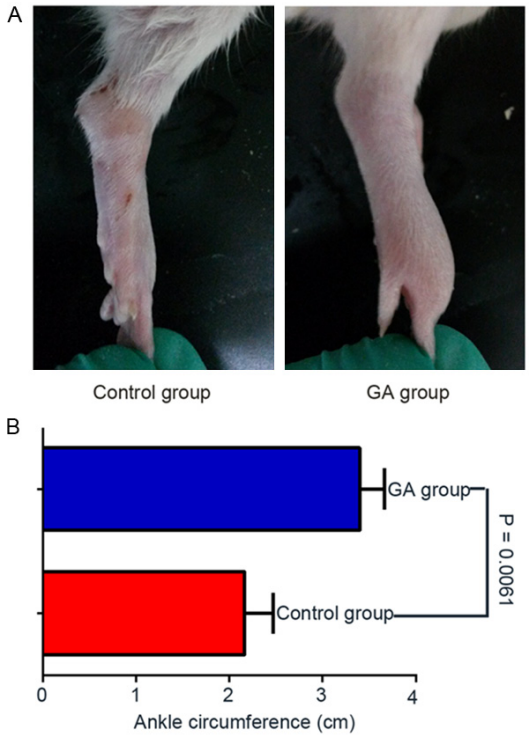

Figure 1. MSU crystals successfully induced acute GA in rat ankles. A. Images of the left ankles of rats underwent MSU solution injection. MSU crystals induced obvious ankle swelling in rats at 24 h. B. The left ankle circumference of each rat was measured. Data were presented as mean ± SD (n = 3).

Results

Successful establishment of GA in rats

In order to evaluate the impacts of MSU crystal injection in rats, the circumferences of their left ankle joints were measured in both control and GA groups at 24 h post-injection. As illustrated in **Figure 1**, a marked increase in ankle joint circumference was found in GA rats (2.2 ± 0.31 cm in Control group vs. 3.4 ± 0.26 cm in GA group; **Figure 1**). The observed ankle swelling induced by MSU crystals indicated the successful establishment of GA in rat ankle.

PCA of the microarray data

PCA is often utilized to decrease the dimension of high-dimensional datasets by assessing sample similarities as well as differences [14]. To estimate whether the six samples used for microarray assay could be distinguished, PCA was thus running in the obtained array data of each sample. We found that the analyzed six

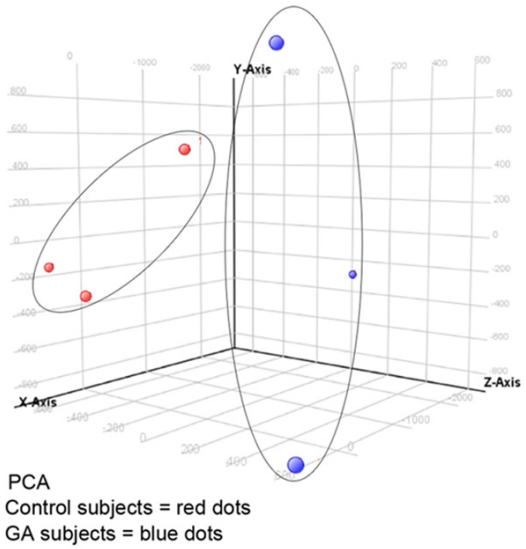

Figure 2. PCA distinguished the experimental rats into two groups. PCA algorithm used to analyze the obtained microarray data. Samples from the similar circumstance seemed to cluster into a group.

samples could be distinguished from each other, and classified into two groups (**Figure 2**).

Identification of differentially expressed miRNAs in rat ankle synovial tissues

Microarray analysis was conducted here to investigate how high-level urate affected miRNA expression in synovial tissues. As shown in the volcano plot image, nine out of the analyzed 728 miRNA had altered expression level (FC > 1 and *P* value < 0.05, **Figure 3A**). Only seven miRNAs had FC > 1.2 and *P* value < 0.05, and thus they were considered as significant differentially expressed miRNAs. Three miRNAs (rno-miR-328b-3p, rno-miR-375-5p, rno-miR-299a-5p) were found to be upregulated in GA synovial tissues, while four (rno-miR-203a-3p, rno-miR-3085, rno-miR-19b-2-5p and rno-miR-741-3p) were downregulated. Unsupervised hierarchical clustering analysis was performed in the 7 differentially expressed miRNAs. Results were shown as a heat map, revealing that samples from the similar condition were clustered (**Figure 3B**). Additionally, qRT-PCR analysis was performed to validate the microarray data. The qRT-PCR results were corresponded to the prior microarray data (**Figure 3C**). However, although the expression of miR-741-3p was slightly decreased in GA synovium, there was no statistical significance (*P* value = 0.889). Therefore, this miRNA was excluded

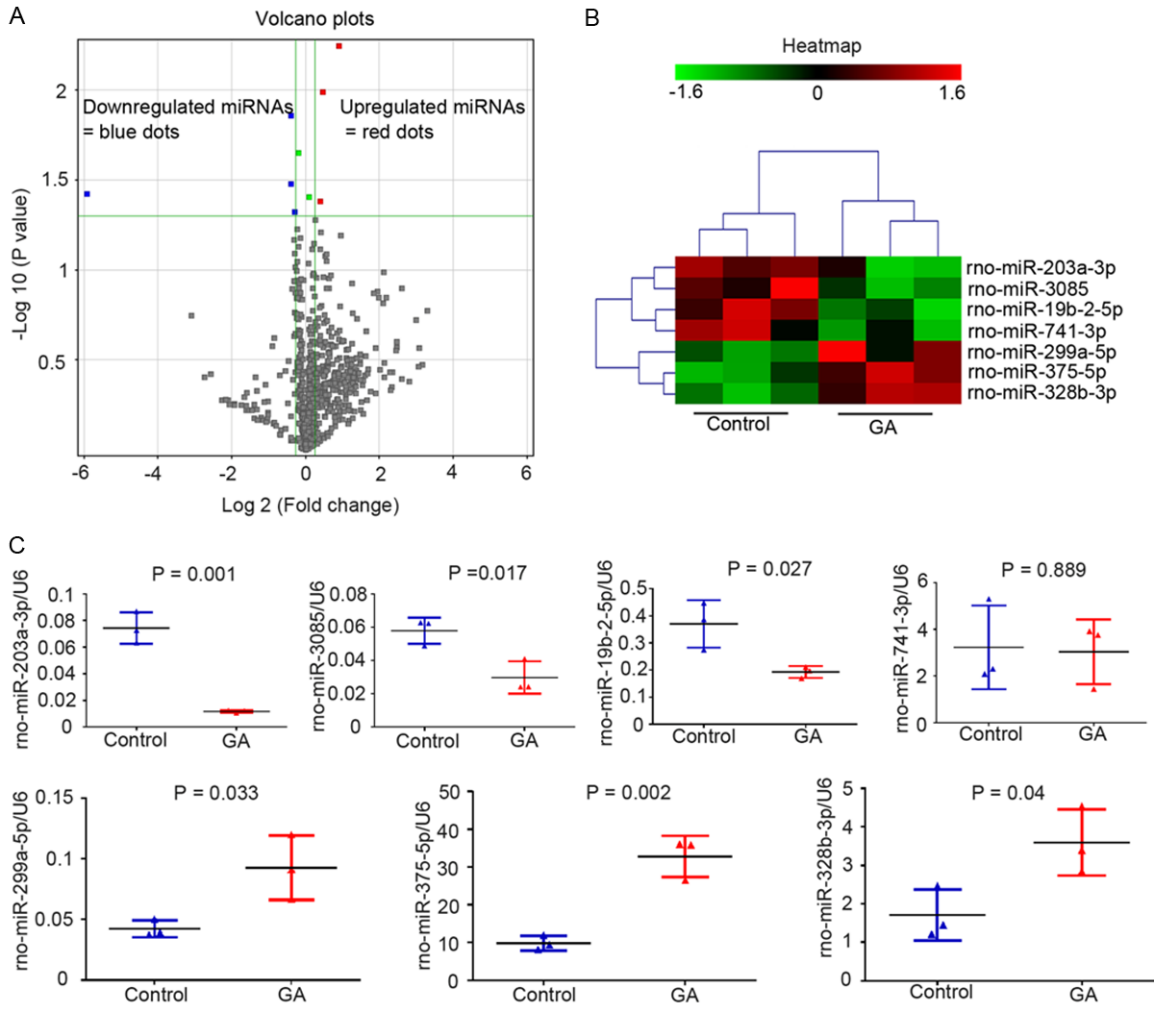

Figure 3. Differentially expressed miRNAs were identified in synovial tissues in rats with GA. A. MiRNAs were plotted in a volcano plot. A dot in blue or red represented a miRNA with the absolute FC > 1.2 and *P* value < 0.05. These miRNAs were considered as differentially expressed. B. Unsupervised hierarchical clustering analysis was performed in the 7 differentially expressed miRNAs, and the results were exhibited in a heat map. Red color in each column indicated the miRNA expression level was higher than the median, while green indicated a lower level. C. QRT-PCR was performed to confirm the prior microarray data. Data were presented as mean ± SD (n = 3), and then analyzed with unpaired *t* test. A *P* value less than 0.05 was considered as statistical significant.

from the subsequent target prediction analysis.

GO annotation and KEGG pathway analysis of putative target genes

MiRNAs directly bind to the 3'UTR region of mRNAs, regulating the corresponding gene expression. To understand the roles of the validated differentially expressed miRNAs in GA, their targets were predicted through miRDB online resource [15]. A GO or pathway item with $P < 0.05$ was considered as significant. We found that, within the biological process, genes targeted by three upregulated miRNAs were mainly enriched in regulation of transcription and negative/positive regulation of apoptotic process (**Table 1**, Supplementary Material 1). Although no information was available about the biological process of 97 genes targeted by the three downregulated miRNAs, the rest target genes were mainly annotated into regulation of transcription, signal transduction, etc. (**Table 2**, Supplementary Material 2). Moreover, genes either targeted by the upregulated or downregulated miRNAs were enriched in several essential molecular functions, such as protein binding, sequence-specific DNA binding,

Table 1. Representative GO items of genes targeted by the upregulated miRNAs (Biological process and Molecular function)

Term ID	Term Description	List Hits	Representative Genes	*P* value
Biological process				
GO:0045944	Positive regulation of transcription from RNA polymerase II promoter	27	TMPRSS6; EBF1; HOXD9; CTCF; MEN1; DDX58	0.0021
GO:0006355	Regulation of transcription, DNA-template	27	MAPK8; PIAS3; EBF1; HBP1; RSL1; HOXD9	0.0047
GO:0006351	Transcription, DNA-template	22	PIAS3; EBF1; HBP1; HOXD9; MAFG; FOXG1	0.0022
GO:0045893	Positive regulation of transcription, DNA-template	21	SFRP1; EBF1; CTCF; MEN1; TP73; MYF6	0.0001
GO:0000122	Negative regulation of transcription from RNA polymerase II promoter	21	TMPRSS6; WDTC1; HIC1; HOXD9; FGF9; FOXG1	0.0029
GO:0045892	Negative regulation of transcription, DNA-template	16	SFRP1; TMPRSS6; FOXG1; CTCF; MEN1; MYF6	0.0060
GO:0042493	Response to drug	15	ABCD3; SFRP1; CYP27B1; TP73; PRSS8; CDK1	0.0119
GO:0008285	Negative regulation of cell proliferation	13	SFRP1; MYO16; NF2; BNIPL; MEN1; CYP27B1	0.0044
GO:0043066	Negative regulation of apoptotic process	13	MAPK8; CCNG1; CDK1; NFKB1; IL2RB; BCL2L2	0.0455
GO:0043065	Positive regulation of apoptotic process	12	MAPK8; TP73; CNR1; TGM2; TCF7L2; PPP2R4	0.0037
Molecular function				
GO:0005515	Protein binding	32	MAPK8; ABCD3; PIAS3; GIPC1; MYO16; NF2	0.0300
GO:0005524	ATP binding	30	MAPK8; ABCD3; MYO19; TESK2; KIF24; RAD51D	0.0339
GO:0046872	Metal ion binding	29	TESK2; ZFP827; HIC1; ZFP704; RSL1; ZFP46	0.0201
GO:0043565	Sequence-specific DNA binding	19	HIC1; HOXD9; MAFG; FOXG1; CTCF; MEN1	0.0008
GO:0003700	Transcription factor activity, sequence-specific DNA binding	18	HIC1; HOXD9; MAFG; FOXG1; CTCF; TP73	0.0191
GO:0042802	Identical protein binding	15	SFRP1; ARFIP1; YWHAZ; BNIPL; SIAH1; DDX58	0.0478
GO:0003676	Nucleic acid binding	15	ZFP827; HIC1; RSL1; ZFP46; AARSD1; CPSF4	0.0297
GO:0003682	Chromatin binding	13	CTCF; MEN1; TP73; ZNF354B; MED1; SETD7	0.0159
GO:0000978	RNA polymerase II core promoter proximal region sequence-specific DNA binding	13	CTCF; TP73; MED1; NR3C1; EBF1; MTF1	0.0020
GO:0008134	Transcription factor binding	12	YWHAZ; ABI1; TP73; MED1; NKX3-1; HDAC4	0.0031

P value is calculated by the unilateral Fisher exact test. List Hits, the number of genes targeted by the upregulated miRNAs within the GO term.

Table 2. Representative Go items of genes targeted by the downregulated miRNAs (Biological process and Molecular function)

Term ID	Term Description	List Hits	Representative Genes	*P* value
Biological process				
GO:0008150	Biological_process	92	CHST5; SORCS3; SLC7A7; RING1; GPN2; TBL1X	0.0227
GO:0006351	Transcription, DNA-template	42	PRKAA1; RING1; PRKCB; MAFF; DR1; TP53INP2	0.0382
GO:0045893	Positive regulation of transcription, DNA-template	38	EGR2; ACVRL1; SFRP1; ARNT2; TBL1X; MED14	0.0036
GO:0006366	Transcription from RNA polymerase II promoter	34	EGR2; ARNT2; SNAI3; SIX4; ATF1; STAG1	0.0020
GO:0007165	Signal transduction	31	IL6ST; ACVRL1; SPARC; ARHGAP28; PRKAB1; ARHGAP42	0.0115
GO:0043547	Positive regulation of GTPase activity	29	DOCK10; ARHGAP42; ARHGEF26; RGL1; ARAP2; MON2	0.0039
GO:0006357	Regulation of transcription from RNA polymerase II promoter	27	ESX1; PRKCB; TBL1X; MED14; TRAK2; SNAI3	0.0364
GO:0007156	Homophilic cell adhesion via plasma membrane adhesion molecules	17	PCDHGA9; CHL1; CDH11; PCDHGB8; PCDHGA7; PVRL1	0.0003
GO:0007264	Small GTPase mediated signal transduction	13	DOCK10; ARL6; YWHAQ; RGL1; ARL13B; NKIRAS1	0.0447
GO:0030335	Positive regulation of cell migration	13	EDN1; FGR; PTP4A1; S1PR1; IRS2; ATP8A1; CXCL12	0.0447
Molecular function				
GO:0005515	Protein binding	89	PRKAR2B; INA; PRKAA1; CACNA2D1; TMPO; GABBR2	0.0023
GO:0046872	Metal ion binding	72	PRKAA1; EGR2; COL11A1; CACNA2D1; ACVRL1; ZFP39	0.0194
GO:0044822	Poly(A) RNA binding	70	CELF1;MTPAP;DHX33;PHF6;TPR;TNRC6B;NOVA1	0.0159
GO:0003700	Transcription factor activity, sequence-specific DNA binding	41	EGR2; ZFP39; MAFF; SNAI3; SIX4; IKZF5	0.0342
GO:0019901	Protein kinase binding	30	PRKAR2B; CACNB4; SLC12A7; ACVRL1; CDC25C; EXOC2	0.0085
GO:0000978	RNA polymerase II core promoter proximal region sequence-specific DNA binding	24	EGR2; SNAI3; SIX4; FOXP2; ONECUT2; DLX5	0.0141
GO:0019904	Protein domain specific binding	22	PRKAR2B; CCNG1; TBL1X; OSBP; MAP1LC3B; TJP1	0.0124
GO:0001077	Transcriptional activator activity, RNA polymerase II core promoter proximal region sequence-specific binding	19	EGR2; SIX4; ONECUT2; BARHL1; DLX5; BCL11B	0.0180
GO:0000977	RNA polymerase II regulatory region sequence-specific DNA binding	16	ESX1; GATAD2A; ZFP39;SNAI3; IKZF5; SOX13	0.0361
GO:0008017	Microtubule binding	14	KIF6; KIF16B; MAP1LC3B; KIF2A; SNCA; CNN3	0.0475

P value is calculated by the unilateral Fisher exact test. List Hits, the number of genes targeted by the downregulated miRNAs within the GO term.

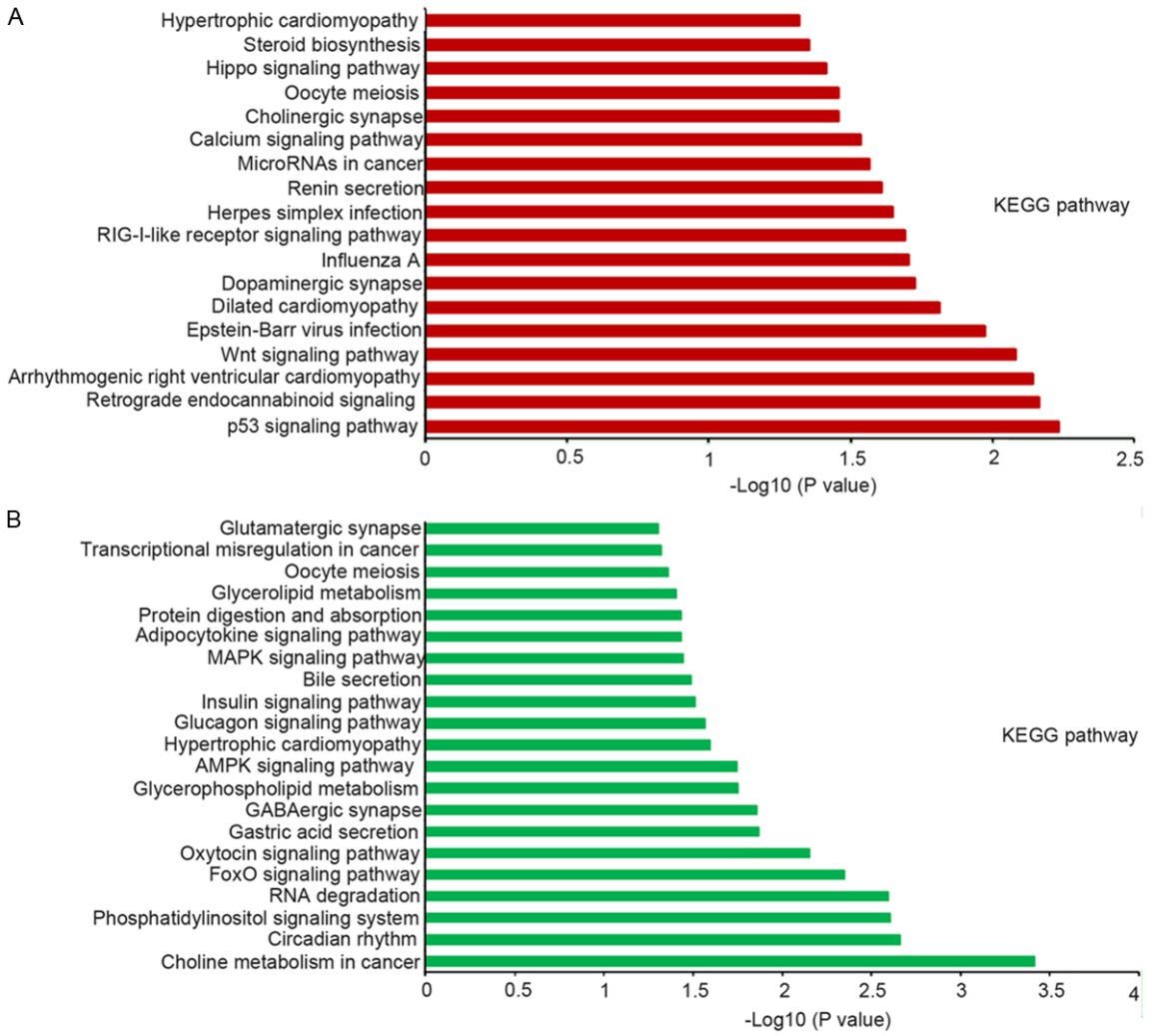

Figure 4. KEGG pathway analysis of the putative targets of six validated miRNAs. MiRDB online database was used to predict the potential targets for the upregulated and downregulated miRNAs, respectively. These target genes were annotated into a variety of essential pathways (A for the upregulated miRNAs; B for the downregulated miRNAs). Bigger -log10 (*P* value) indicated a smaller *P* value.

ATP binding, metal ion binding, etc. (**Tables 1** and **2**, Supplementary Materials 3 and 4).

Pathways regulated by the upregulated and downregulated miRNAs were analyzed. As indicated in **Figure 4**, the most significant signaling transduction pathway mediated by the upregulated miRNAs was p53 pathway, a well-known apoptosis related pathway (**Figure 4A**). The downregulated miRNA-targeted genes were found to be enriched in RNA degradation, FoxO signaling pathway, MAPK signaling pathway, etc. (**Figure 4B**).

Discussion

MSU crystals trigger an acute inflammatory reaction in GA patients, and are detectable in the synovial fluids even after the inflammation resolution [16]. MiRNA dysregulation is link to the pathogenesis of arthritis, including RA and OA as evidenced by plenty of previous studies [17, 18]. However, studies on the association of miRNAs and GA are relatively scarce. Therefore, to gain insights into the association between miRNAs and GA pathogenesis, miRNA array analysis was performed to assess the miRNA expression profile in synovial tissues of control and MSU-induced GA rats. Genes targeted by the validated differentially expressed miRNAs were subjected to subsequent bioinformatics analysis.

GA was first induced in rats by directly injecting MSU crystals into the ankle joint cavity. An obvi-

ous ankle joint edema was observed in these rats. Application of miRNA microarrays enabled us to assess the expression of 728 rat miRNAs (the complete mature rat miRNA sequences in miRBase release 20.0) in rat synovial tissues. The PCA and unsupervised hierarchical clustering analyses indicated a proper grouping of the 6 analyzed samples. The array data were additionally validated by qRT-PCR, and the results showed that miR-328b-3p, miR-375-5p and miR-299a-5p were upregulated in ankle synovial tissues in response to MSU crystal injection, whereas miR-203a-3p, miR-3085 and miR-19b-2-5p were downregulated. Finding the correlation of these dysregulated miRNAs with inflammation may be the key to understand the miRNA-related GA pathogenesis.

Neutrophil activation stimulated by MSU crystals leads to the overproduction of the superoxides and pro-inflammatory cytokines and the formation of the neutrophil extracellular traps, exacerbating the inflammatory process [19]. The apoptosis of neutrophils and the uptake of MSU crystals by macrophages can promote the resolution of gouty inflammation [19, 20]. MiR-328b-3p is a member of miR-328a/328b-3p family, whose expression was found to be significantly increased in GA synovial tissues in this study. Interestingly, antagonism of miR-328 enhances the function of macrophages and neutrophils to clear the pathogenic bacteria in mouse lung [21]. It is likely that inhibiting the aberrant elevation of miR-328b-3p may promote the host defense responses against MSU crystal stimulation. Additionally, non-inflammatory monocytes can be recruited by MSU crystals to differentiate into M1-like pro-inflammatory macrophages in murines with peritoneal gout [22]. Whether miR-328b-3p is implicated MSU-mediated macrophage differentiation requires for further investigation.

Recently, Miao and co-workers found that miR-375-3p (previously name miR-375) was decreased in fibroblast-like synoviocytes derived from RA rats, and that increasing the miR-375-3p expression could attenuate arthritis in these rats [23]. This previous finding suggested a protective role of miR-375-3p in arthrophlogosis. Of note, both miR-375-3p and miR-375-5p were generated from mir-375, but they have different seed sequences. Although no significant change of miR-375-3p was observed in GA synovium, miR-375-5p was found to be upregulated. To our best knowledge, miR-375-5p was identified as a differentially expressed miRNA in synovial tissues in response to MSU crystal stimulation for the first time, and so was miR-299a-5p. Further experiments using the mimics or antago-miRNAs of these two miRNAs will help to understand their roles in GA pathogenesis.

Reportedly, miR-203a-3p (previously name miR-203) directly targets myeloid differentiation factor 88 (MyD88), and subsequently inhibits MyD88 downstream signals, such as nuclear factor kappa B 1 (NF-κB1), TNF-α and interleukin-6 (IL-6) in mouse RAW264.7 cells [24]. Likewise, miR-203a-3p also inhibits the inflammatory responses in microglial cells by suppressing NF-κB signaling [25]. Contrarily, Stanczyk and colleagues demonstrates that miR-203a-3p promotes matrix metalloproteinases 1 (MMP1) and IL-6 release in human RA synovial fibroblasts, which is dependent on NF-κB signaling activation [26]. However, unlike the former two studies, no direct miR-203 targets were identified in the latter study. Besides, NOD-like receptor (NLR) family pyrin domain-containing 1A (NLRP1A) is a potential target of miR-203a-3p, whose activation can drive the formation of inflammasomes [27]. MSU crystals have been found to trigger inflammation by activating of the NLRP inflammasomes [28]. Herein, we found that miR-203a-3p was significantly decreased in GA synovial tissues. We thus proposed that the reduction of miR-203a-3p was linked to the activation of NLRP inflammasomes, and that restoring the decreased miR-203a-3p might inhibit NLRP-mediated inflammation in GA. This hypothesis is currently being tested in our lab.

MiR-3085, a newly identified chondrocyte-selective miRNA, can directly target alpha 5-integrin (ITGA5), and thus is suggested to affect the cartilage homeostasis and OA [29]. Bone remodeling in chronic gout is link to MSU crystal deposits, in which beta 2-integrin (ITGB2)-mediated neutrophil adhesion to MSU-activated osteoblasts plays a critical role [30]. Interestingly, besides ITGA5, we found that genes encoding other integrin subunits, such as ITGA9 and ITGA10, were also potential targets of miR-3085. Elucidation of the interaction between the decreased miR-3085 with its tar-

get integrin genes may help to reveal the underlying mechanisms of MSU crystal-mediated neutrophil adhesion.

MiR-19a-3p (previously name miR-19a) and miR-19b-3p (previously name miR-19b) belong to the same cluster and share the same seed sequence (3'AAACGUG5'). Philippe et al. found that miR-19a/b mimics decreased toll-like receptor 2 (TLR2) expression level, and suppressed IL-6 and MMP 3 secretion in activated fibroblast-like synoviocytes [31]. This previous research indicated miR-19a/b as negative regulators of inflammation. But such findings are disproved by Gantier and co-workers latter [32]. They contrarily showed that miR-19b mimics could exacerbate the inflammatory activation in fibroblast-like synoviocytes by potentiating NF-κB activity, revealing miR-19b as a contributor to the pathology of arthritis. In the present study, although both rno-miR-19a-3p and rno-miR-19b-3p were increased in MSU-treated synovial tissues, no statistical significances were observed. Nonetheless, we found that miR-19b-2-5p (miR-19b-2*) was marked decreased in pathological synovial tissues. Although miR-19b-5p has a different seed sequence (3'GUUUUG 5') from miR-19a/b-3p, these miRNAs are all generated from the miR-19 precursor. As far as we know, our study was the first to show a dysregulation of miR-19b-5p in gout-related arthritis.

Further Go annotation and pathway analysis were performed to investigate how the upregulated and downregulated miRNAs participated in GA. We found that the apoptotic process, more specific, the p53 signaling might be mediated by the three upregulated miRNAs. P53 promotes the pro-apoptotic pathway in response to DNA damage stimuli, and has gained intensive attention in the field of carcinogenesis [33]. Licandro and co-workers have found that MSU crystals induce inflammatory responses in murine dendritic cells by promoting NLRP3 inflammasome-mediated p53 signaling activation [34]. Furthermore, genes targeted by the three downregulated miRNAs were mainly involved in inflammation or oxidative stress related pathway such as MAPK and FoxO signaling pathways. Though beyond the scope of the present study, it will be interesting to investigate how the dysregulated miRNAs function through the above mentioned GA-related pathways.

In this study, a dysregulation of miRNAs has been found in ankle synovial tissues of rats with MSU crystal-induced GA. Three upregulated miRNAs (miR-328b-3p, miR-375-5p and miR-299a-5p) and three downregulated miRNAs (miR-203a-3p, miR-3085 and miR-19b-2-5p) were identified and validated in GA synovial tissues. These miRNAs are promising therapeutic molecules or targets for GA.

Acknowledgements

This study was supported by a grant from the National Natural Science Foundation of China (No. 81173170).

Disclosure of conflict of interest

None.

Address correspondence to: Dr. Deyou Jiang, Department of Synopsis of The Golden Chamber, School of Basic Medical Sciences, Heilongjiang University of Chinese Medicine, 24 Heping Road, Harbin 150040, People's Republic of China. Tel: +86-451-82193627; Fax: +86-451-82193627; E-mail: deyou_jiang@126.com

References

[1] Jordan KM. Up-to-date management of gout. Curr Opin Rheumatol 2012; 24: 145-151.
[2] ten Klooster PM, Vonkeman HE and van de Laar MA. Disability due to gouty arthritis. Curr Opin Rheumatol 2012; 24: 139-144.
[3] Biscaglia S, Ceconi C, Malagu M, Pavasini R and Ferrari R. Uric acid and coronary artery disease: An elusive link deserving further attention. Int J Cardiol 2015; [Epub ahead of print].
[4] Harrold L. New developments in gout. Curr Opin Rheumatol 2013; 25: 304-309.
[5] Dumusc A and So A. Interleukin-1 as a therapeutic target in gout. Curr Opin Rheumatol 2015; 27: 156-163.
[6] Janssens HJ, Janssen M, van de Lisdonk EH, van Riel PL and van Weel C. Use of oral prednisolone or naproxen for the treatment of gout arthritis: a double-blind, randomised equivalence trial. Lancet 2008; 371: 1854-1860.
[7] Dalbeth N, Lauterio TJ and Wolfe HR. Mechanism of action of colchicine in the treatment of gout. Clin Ther 2014; 36: 1465-1479.
[8] Chandradoss SD, Schirle NT, Szczepaniak M, MacRae IJ and Joo C. A Dynamic Search Process Underlies MicroRNA Targeting. Cell 2015; 162: 96-107.

[9] Jonas S and Izaurralde E. Towards a molecular understanding of microRNA-mediated gene silencing. Nat Rev Genet 2015; 16: 421-433.
[10] Ammari M, Jorgensen C and Apparailly F. Impact of microRNAs on the understanding and treatment of rheumatoid arthritis. Curr Opin Rheumatol 2013; 25: 225-233.
[11] Beyer C, Zampetaki A, Lin NY, Kleyer A, Perricone C, Iagnocco A, Distler A, Langley SR, Gelse K, Sesselmann S, Lorenzini R, Niemeier A, Swoboda B, Distler JH, Santer P, Egger G, Willeit J, Mayr M, Schett G and Kiechl S. Signature of circulating microRNAs in osteoarthritis. Ann Rheum Dis 2015; 74: e18.
[12] Dalbeth N, Pool B, Shaw OM, Harper JL, Tan P, Franklin C, House ME, Cornish J and Naot D. Role of miR-146a in regulation of the acute inflammatory response to monosodium urate crystals. Ann Rheum Dis 2015; 74: 786-790.
[13] Jin HM, Kim TJ, Choi JH, Kim MJ, Cho YN, Nam KI, Kee SJ, Moon JB, Choi SY, Park DJ, Lee SS and Park YW. MicroRNA-155 as a proinflammatory regulator via SHIP-1 down-regulation in acute gouty arthritis. Arthritis Res Ther 2014; 16: R88.
[14] Sanguinetti G, Milo M, Rattray M and Lawrence ND. Accounting for probe-level noise in principal component analysis of microarray data. Bioinformatics 2005; 21: 3748-3754.
[15] Wong N and Wang X. miRDB: an online resource for microRNA target prediction and functional annotations. Nucleic Acids Res 2015; 43: D146-152.
[16] Schauer C, Janko C, Munoz LE, Zhao Y, Kienhofer D, Frey B, Lell M, Manger B, Rech J, Naschberger E, Holmdahl R, Krenn V, Harrer T, Jeremic I, Bilyy R, Schett G, Hoffmann M and Herrmann M. Aggregated neutrophil extracellular traps limit inflammation by degrading cytokines and chemokines. Nat Med 2014; 20: 511-517.
[17] Salehi E, Eftekhari R, Oraei M, Gharib A and Bidad K. MicroRNAs in rheumatoid arthritis. Clin Rheumatol 2015; 34: 615-628.
[18] Le LT, Swingler TE and Clark IM. Review: the role of microRNAs in osteoarthritis and chondrogenesis. Arthritis Rheum 2013; 65: 1963-1974.
[19] Mitroulis I, Kambas K and Ritis K. Neutrophils, IL-1beta, and gout: is there a link? Semin Immunopathol 2013; 35: 501-512.
[20] Scott P, Ma H, Viriyakosol S, Terkeltaub R and Liu-Bryan R. Engagement of CD14 mediates the inflammatory potential of monosodium urate crystals. J Immunol 2006; 177: 6370-6378.
[21] Tay HL, Kaiko GE, Plank M, Li J, Maltby S, Essilfie AT, Jarnicki A, Yang M, Mattes J, Hansbro PM and Foster PS. Antagonism of miR-328 increases the antimicrobial function of macrophages and neutrophils and rapid clearance of non-typeable Haemophilus influenzae (NTHi) from infected lung. PLoS Pathog 2015; 11: e1004549.
[22] Martin WJ, Shaw O, Liu X, Steiger S and Harper JL. Monosodium urate monohydrate crystal-recruited noninflammatory monocytes differentiate into M1-like proinflammatory macrophages in a peritoneal murine model of gout. Arthritis Rheum 2011; 63: 1322-1332.
[23] Miao CG, Shi WJ, Xiong YY, Yu H, Zhang XL, Qin MS, Du CL, Song TW and Li J. miR-375 regulates the canonical Wnt pathway through FZD8 silencing in arthritis synovial fibroblasts. Immunol Lett 2015; 164: 1-10.
[24] Wei J, Huang X, Zhang Z, Jia W, Zhao Z, Zhang Y, Liu X and Xu G. MyD88 as a target of microRNA-203 in regulation of lipopolysaccharide or Bacille Calmette-Guerin induced inflammatory response of macrophage RAW264.7 cells. Mol Immunol 2013; 55: 303-309.
[25] Yang Z, Zhong L, Zhong S, Xian R and Yuan B. miR-203 protects microglia mediated brain injury by regulating inflammatory responses via feedback to MyD88 in ischemia. Mol Immunol 2015; 65: 293-301.
[26] Stanczyk J, Ospelt C, Karouzakis E, Filer A, Raza K, Kolling C, Gay R, Buckley CD, Tak PP, Gay S and Kyburz D. Altered expression of microRNA-203 in rheumatoid arthritis synovial fibroblasts and its role in fibroblast activation. Arthritis Rheum 2011; 63: 373-381.
[27] Dowling JK and O'Neill LA. Biochemical regulation of the inflammasome. Crit Rev Biochem Mol Biol 2012; 47: 424-443.
[28] Ghaemi-Oskouie F and Shi Y. The role of uric acid as an endogenous danger signal in immunity and inflammation. Curr Rheumatol Rep 2011; 13: 160-166.
[29] Crowe N, Swingler TE, Le LT, Barter MJ, Wheeler G, Pais H, Donell ST, Young DA, Dalmay T and Clark IM. Detecting new microRNAs in human osteoarthritic chondrocytes identifies miR-3085 as a human, chondrocyte-selective, microRNA. Osteoarthritis Cartilage 2016; 24: 534-43.
[30] Allaeys I, Rusu D, Picard S, Pouliot M, Borgeat P and Poubelle PE. Osteoblast retraction induced by adherent neutrophils promotes osteoclast bone resorption: implication for altered bone remodeling in chronic gout. Lab Invest 2011; 91: 905-920.
[31] Philippe L, Alsaleh G, Suffert G, Meyer A, Georgel P, Sibilia J, Wachsmann D and Pfeffer S. TLR2 expression is regulated by microRNA miR-19 in rheumatoid fibroblast-like synoviocytes. J Immunol 2012; 188: 454-461.

[32] Gantier MP, Stunden HJ, McCoy CE, Behlke MA, Wang D, Kaparakis-Liaskos M, Sarvestani ST, Yang YH, Xu D, Corr SC, Morand EF and Williams BR. A miR-19 regulon that controls NF-kappaB signaling. Nucleic Acids Res 2012; 40: 8048-8058.

[33] Yoon KW, Byun S, Kwon E, Hwang SY, Chu K, Hiraki M, Jo SH, Weins A, Hakroush S, Cebulla A, Sykes DB, Greka A, Mundel P, Fisher DE, Mandinova A and Lee SW. Control of signaling-mediated clearance of apoptotic cells by the tumor suppressor p53. Science 2015; 349: 1261669.

[34] Licandro G, Ling Khor H, Beretta O, Lai J, Derks H, Laudisi F, Conforti-Andreoni C, Liang Qian H, Teng GG, Ricciardi-Castagnoli P and Mortellaro A. The NLRP3 inflammasome affects DNA damage responses after oxidative and genotoxic stress in dendritic cells. Eur J Immunol 2013; 43: 2126-2137.